If $(n_x, n_y) = (0, 1)$, we have

$$N_X = 0 \tag{47}$$

$$N_Y = 1 \tag{48}$$

$$\Psi^* = 1 \tag{49}$$

Substitute these two special cases (44–49) into Eq. (43). The solutions for anisotropic material can be obtained from the corresponding isotropic problem in Cartesian coordinate as follows:

$$w^a(x, y) = (\mu/C)w^i(X, Y) \tag{50}$$

$$\tau^a_{yz}(x, y) = \tau^i_{YZ}(X, Y) \tag{51}$$

$$\tau^a_{xz}(x, y) = (1/c_{44})\left[C\tau^i_{XZ}(X, Y) + c_{45}\tau^i_{YZ}(X, Y)\right] \tag{52}$$

The anisotropic antiplane problems can be converted into the one involving isotropic materials by properly changing the geometry and the tractions on the boundary. The procedure may be indicated as follows:

1) The geometry of the original anisotropic problem is changed to the corresponding isotropic problem by using Eqs. (34) and (35) in a polar coordinate system or using Eqs. (36) and (37) in a Cartesian coordinate system.

2) The boundary tractions are changed by Eq. (40). Note that the total force produced by the traction for the anisotropic problem is the same as that for the corresponding isotropic problem after transformation.

3) Solve the associated isotropic problem.

4) The relationship shown in Eqs. (31–33) for polar coordinates or Eqs. (50–52) for Cartesian coordinates is used to obtain the displacement and shear stresses for the anisotropic problem.

## Conclusions

Solving an isotropic problem has always been easier than the corresponding anisotropic problem in both the analytical analysis and the numerical investigation. The antiplane problem of anisotropic materials is investigated in detail. In analytical studies, solutions of antiplane problems have served two distinct purposes. First, they could be used for shedding some light on the qualitative behavior of the solutions for somewhat more difficult inplane problems. Second, they could have practical applications in their own right in situations such as relationship for the full-field solutions of stress and displacement between the anisotropic materials and the corresponding isotropic problems have been established. Through such a correspondence, solutions for anisotropic problems could be expressed in terms of those for isotropic problems. With this correspondence at hand, investigating the complicated antiplane anisotropic problem has become very convenient. Attention needs, therefore, only be focused on the problem of isotropic materials.

## Acknowledgment

The financial support by the National Science Council, Republic of China, through Grant NSC 79-0401-E-002-37 to National Taiwan University is gratefully acknowledged.

## References

[1]Williams, M. L., "Stress Singularities Resulting from Various Boundary Conditions in Angular Corners of Plates in Extension," *Journal of Applied Mechanics*, Vol. 19, No. 4, 1952, pp. 526–528.

[2]Tranter, C. J., "Use of the Mellin Transform in Finding the Stress Distribution in an Infinite Wedge," *Quarterly Journal of Mechanics and Applied Mathematics*, Vol. 1, No. 2, 1948, pp. 125–130.

[3]Stroh, A. N., "Dislocations and Cracks in Anisotropic Elasticity," *Philosophical Magazine*, Vol. 3, 1958, pp. 625–646.

[4]Ting, T. C. T., "Explicit Solution and Invariance of the Singularities at an Interface Crack in Anisotropic Composites," *International Journal of Solids and Structures*, Vol. 22, No. 9, 1986, pp. 965–983.

[5]Bogy, D. B., "Plane Solution for Anisotropic Elastic Wedges under Normal and Shear Loading," *Journal of Applied Mechanics*, Vol. 39, No. 4, 1972, pp. 1103–1109.

[6]Ma, C. C., and Hour, B. L., "Analysis of Dissimilar Anisotropic Wedges Subjected to Antiplane Shear Deformation," *International Journal of Solids and Structures*, Vol. 25, No. 11, 1989, pp. 1295–1309.

[7]Ma, C. C., "Antiplane Problems of Monoclinic Material," *Journal of Engineering Mechanics*, Vol. 118, No. 9, 1992, pp. 1765–1782.

# Inclusion of Transverse Shear Deformation in Optimum Design of Aircraft Wing Panels

Phil W. L. Williams,* Fred W. Williams,† and David Kennedy‡
*University of Wales,*
*Cardiff CF2 1XH, Wales, United Kingdom*

## Introduction

THE effects of shear deformation plate theory (SDPT) on the minimum mass design of composite prismatic plate assemblies of practical aircraft wing panel proportions are investigated using VICONOPT.[1] Critical buckling loads for single plates calculated using SDPT are lower than those calculated using classical plate theory (CPT), the difference often being significant for thick laminates. For plate assemblies,[2] material properties and the relative thicknesses cause greater SDPT vs CPT differences for local buckling modes than for overall ones. The differences are particularly large for sandwich panels with low density foam cores,[3] but the present Note addresses thick laminate cases only.

In the optimum designs presented, the panel mass is minimized subject to buckling, ply strain, and geometric constraints. Design variables include plate breadths and individual ply thicknesses. The results compare SDPT and CPT and use VIPASA[4] or VICON[5] buckling analysis as appropriate, both of which require the calculation, at every longitudinal half-wavelength $\lambda$ and at every iteration of the Wittrick–Williams algorithm,[4] of the transcendental stiffness matrix $\boldsymbol{k}$ for a flat plate carrying in-plane longitudinal ($N_x$), transverse ($N_y$), and shear ($N_{xy}$) loads per unit length of their edges. The CPT used assumes a balanced, symmetric laminate and the absence of through thickness shear strains, so that normals to the centroidal plane remain so after deformation. The SDPT used is first order,[3] i.e., normals remain straight but not normal after deformation.

Nondimensional parameters $\beta$ and $\mu$ represent the degradations in critical buckling load and optimum mass, respectively, because SDPT is used instead of CPT. Thus, if SDPT is used to analyze a CPT design, the panel fails to carry the design load $P$ by a percentage $\beta$, i.e., it carries only $P(1-\beta/100)$. SDPT redesign raises the critical buckling load to $P$ but increases the mass $M$ by a percentage $\mu$, i.e., to $M(1+\mu/100)$.

## Scope of Study

Figure 1 shows a plan view of a benchmark 45 deg swept composite wing skin recently studied by the Group for Aeronautical Research and Technology in Europe (GARTEUR) Working Group on Structural Optimization.[6] The panel P8 shown is the most heavily loaded panel and was designed by VICONOPT to satisfy buckling, strength, and geometric conditions for three load cases. Figure 2 gives the geometric and layup details for panel P8, the ply properties being $E_{11} = 125$ GPa, $E_{22} = 8.8$ GPa, $G_{12} = G_{13} = 5.3$ GPa, $G_{23} = 0.5\ G_{13} = 2.65$ GPa, $\upsilon_{12} = 0.35$, and density $= 1620$ kg/m$^3$.

Received Feb. 24, 1996; accepted for publication July 11, 1996; also published in *AIAA Journal on Disc*, Volume 2, Number 1. Copyright © 1996 by the American Institute of Aeronautics and Astronautics, Inc. All rights reserved.

*Research Associate, Cardiff School of Engineering.

†Professor, Head of Structures, Cardiff School of Engineering. Member AIAA.

‡Lecturer, Cardiff School of Engineering. Member AIAA.

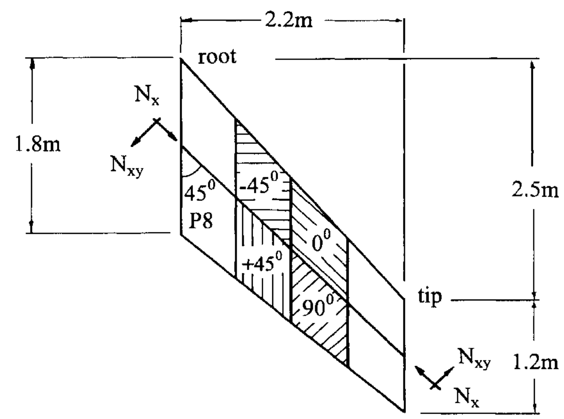


**Fig. 1 Plan view of top skin of benchmark wing, showing ply orientations.**

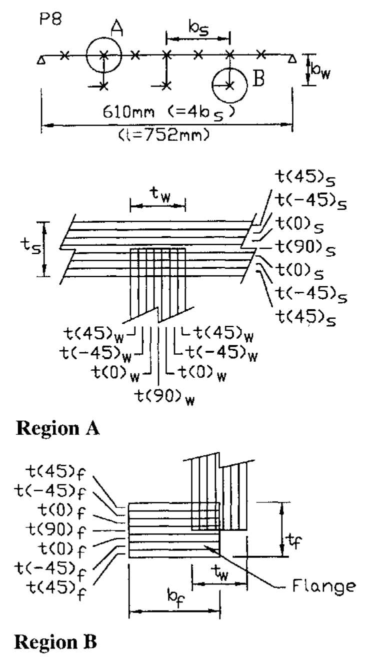


**Fig. 2 Panel P8, showing ply orientations in regions A and B. The stiffener flanges are present for *J* stiffeners and absent for blade stiffeners.**

Crosses denote point supports needed for VICON analysis to represent end conditions by preventing out-of-plane skin or stiffener web deflections.

The present study removes the height constraint for panel P8 so that, unlike in the GARTEUR studies, local buckling will occur at the design load for at least some of the variants of panel P8 considered, so that SDPT becomes important. Variants show the effects of making the panels skewed or of altering material properties, stiffener type and pitch, type and number of loading conditions, and ply strain constraints.

## Results

All results that follow are for panels of length $\ell$ and having rectangular plan unless stated to be skewed. The first variant of panel P8 modeled by VICONOPT[1] had *J* stiffeners, with the stiffener web, flange, and skin constrained to have identical layups. An axial compression load case with the design compressive force $P = 2.558$ MN was chosen to cause an axial panel strain of approximately 0.006 (0.6%), i.e., the maximum ply strain was 0.6% and was in the 0 deg ply. The VIPASA analysis[4] option of VICONOPT was used.

The CPT/SDPT results of Table 1 give the minimum value of the critical buckling load factor $F$ as 0.931 at $\lambda = \ell/5$, so that $\beta = 6.9\%$ and the panel buckles at 93.1% of its design load, i.e., at $FP = 2.381$ MN. However, Table 2 shows that $\mu = 2.4\%$. Hence, using CPT instead of SDPT achieves only a modest mass saving but

**Table 1 $F$ vs $\lambda$ for axially loaded *J* stiffened panel**

| | Design/analysis | | |
|---|---|---|---|
| $\lambda$ | CPT/CPT | CPT/SDPT | SDPT/SDPT |
| $\ell$ | 1.000 | 0.995 | 1.000 |
| $\ell/2$ | 1.233 | 1.211 | 1.282 |
| $\ell/3$ | 1.134 | 1.088 | 1.158 |
| $\ell/4$ | 1.033 | 0.973 | 1.042 |
| $\ell/5$ | 1.000 | 0.931 | 1.000 |
| $\ell/6$ | 1.022 | 0.941 | 1.014 |
| $\ell/7$ | 1.082 | 0.986 | 1.063 |
| $\ell/8$ | 1.170 | 1.054 | 1.138 |
| $\ell/9$ | 1.282 | 1.141 | 1.233 |
| $\ell/10$ | 1.414 | 1.241 | 1.343 |

**Table 2 CPT and SDPT designs for axially loaded *J* stiffened panel**

| Quantity | CPT | SDPT | % change |
|---|---|---|---|
| $t(45)_{w,f,s}$, mm | 0.786 | 0.787 | +0.1 |
| $t(0)_{w,f,s}$, mm | 1.697 | 1.773 | +4.5 |
| $t(90)_{w,f,s}$, mm | 0.207 | 0.239 | +15.4 |
| $t_{w,f,s}$, mm | 6.745 | 6.931 | +2.8 |
| $b_w$, mm | 53.30 | 52.22 | −2.0 |
| $b_f$, mm | 25.00 | 25.00 | 0.0 |
| Mass, kg | 6.942 | 7.107 | +2.4(= $\mu$) |
| Design cycles | 12 | 10 | —— |
| Strain, % | 0.609 | 0.587 | −3.6 |

can have a significant adverse effect on structural stability. Comparison of the columns headed CPT/CPT and CPT/SDPT in Table 1 shows that the greatest differences between CPT and SDPT analysis occurred at short half-wavelengths, i.e., for $\lambda \leq \ell/4$.

Replacing the *J* stiffeners of Tables 1 and 2 with blades, for the same axial design load, caused a reduced panel (and maximum ply) strain of 0.545% for CPT design and of 0.540% for SDPT design. This gave $\beta = 3.8\%$ at $\lambda = \ell/4$ and $\mu = 1.1\%$, compared with the Tables 1 and 2 results of $\beta = 6.9\%$ at $\lambda = \ell/5$ and $\mu = 2.4\%$. The skin thickness was higher than the 6.745 mm of Table 2, being 7.379 mm. Therefore, increasing the thickness of a plate that buckles locally clearly does not always cause $\beta$ to increase, presumably due to the differing skin edge fixity offered by the *J* stiffeners and the associated smaller value of $t(0)_{w,f,s}/t_{w,f,s}$ for Table 2 than for the three-blade case, namely $1.697/6.745 = 0.252$ compared with $2.088/7.379 = 0.283$.

To investigate the effect of multiple load conditions on design, three load cases were used simultaneously for which the values of $\{P$ (kN), $N_y$(N/mm), $N_{xy}$(N/mm)$\}$ were, respectively, {1354.9, 378.4, −643.7}, {1705.2, 240.6, −187.7}, and {795.0, 268.7, −420.7}. Independent skin and blade thicknesses were allowed, and a blade inclination of 87.7 deg, not 90 deg, was used to be consistent with the earlier GARTEUR results. Half-wavelengths of $\lambda = \ell/4$, $\ell/5$, $\ell/6$, $\ell/7$, and $\ell/8$ were used to account for local buckling, and VICON analysis was used to cover overall panel failure modes. Note that $\beta$ was calculated using the lowest $F$ for CPT analysis of any of the three load cases and the lowest $F$ for any of the three SDPT analyses. A low ply strain of 0.395% was obtained, because $N_{xy}$ and $N_y$ were large, with $\mu = 1.0\%$ and $\beta = 4.3\%$ at $\lambda = \ell/5$.

Table 3 shows the effects of adding a ply strain constraint of between 0.2 and 0.4% to the design. The mode was categorized as overall if it had a substantial component with $\lambda = \ell$ and otherwise as local. Results with superscript 1 are for cases for which modes were overall for both CPT and SDPT analyses, giving small $\beta$. Superscript 2 denotes cases for which SDPT governing modes only were local, so that $\beta$ could be quite large. Superscript 3 denotes cases for which the governing mode was local for both CPT and SDPT analyses. The first two rows of Table 3 are for the same problem as the preceding paragraph except for the axial strain constraint and the possible omission of $N_y$. The next pair of rows repeats these results with the material changed for the entire panel to IM7/5260 material[7] for which $E_{11} = 153$ GPa, $E_{22} = 9.0$ GPa, $G_{12} = 5.1$ GPa, $G_{13} = 3.8$ GPa, $G_{23} = 3.3$ GPa, and $\upsilon_{12} = 0.29$. The remaining

**Table 3 Effect of percent allowable ply strain on $\beta$ and $\mu$ for different loadings, material, number of blades, and skew angles**

| | | $\beta$ for % strain | | | $\mu$ for % strain | | |
|---|---|---|---|---|---|---|---|
| $N_y = 0$? | Comment | 0.2 | 0.3 | 0.4 | 0.2 | 0.3 | 0.4 |
| No | —— | $1.0^1$ | $2.9^2$ | $4.4^2$ | 0.0 | 0.7 | 1.2 |
| Yes | —— | $2.3^2$ | $2.7^2$ | $4.7^2$ | 0.0 | 0.1 | 1.1 |
| No | IM7/5260 | $0.6^1$ | $3.5^2$ | $4.6^3$ | 0.3 | 0.1 | 1.0 |
| Yes | IM7/5260 | $0.4^1$ | $3.2^2$ | $5.0^3$ | 0.0 | 0.7 | 1.8 |
| No | Five blades | $0.9^1$ | $3.3^2$ | $3.7^2$ | 0.0 | 0.2 | 0.6 |
| Yes | Five blades | $0.5^1$ | $0.1^1$ | $2.6^2$ | 0.1 | 0.1 | 0.2 |
| No | 15 deg skew | $0.9^1$ | $0.3^1$ | $2.2^1$ | 0.0 | 0.0 | 0.9 |
| No | 45 deg skew | $2.5^1$ | $2.9^2$ | $3.0^2$ | 0.1 | 0.0 | 0.9 |

rows cover the use of five-blade stiffeners instead of three (so in Fig. 2 $b_s$ becomes 101.7 mm) or of analyzing the panel as skewed, with the skew angle defined such that 0 deg is a rectangular panel.

The values $\beta = 2.2$ and 2.5% for the skewed panels are surprisingly high because the mode is overall (superscript = 1). However, a plot of the SDPT mode for the 15 deg skew case demonstrated a mode as much like local as overall, because the dominant half-wavelength across the panel width was small. The same was not true for the 45 deg skew case, for which the high value $\beta = 2.5\%$ was surmised to occur because it is the widthwise out-of-plane stiffness of the skin that causes overall buckling loads of stiffened panels to differ from wide strut theory results. This effect is clearly influenced by using SDPT instead of CPT and is greatest when the skin between longitudinal line supports has to support only a small number of stiffeners, i.e., three in this example, as was confirmed by the answer $\beta = 1.2\%$ given by increasing the number of blade stiffeners to seven for the same load condition but with the panel width doubled.

## Conclusions

The principal conclusion is that the use of SDPT instead of CPT has a substantial effect only for those panels for which local buckling is critical for at least one of the following: the optimum CPT design, the optimum SDPT design, and the SDPT analysis of an optimum CPT design. A major conclusion is that the design of laminated panels by SDPT instead of CPT adds very little to the mass of the panel, i.e., $\mu$ is small. All other things being equal, $\beta$ is higher for designs with thick skins, low out-of-plane shear moduli, high design loads, high permissible ply strains or stresses, thick stiffeners, panels with few stiffeners, and types of stiffener that give substantial rotational constraint to the skin. These qualitative conclusions are drawn from the results presented, which can be used to give a quantitative feel to the conclusions.

## Acknowledgments

The first author acknowledges financial support from the Engineering and Physical Sciences Research Council under Grant GR/J79430. The work has also benefited from useful discussions with M. S. Anderson of NASA Langley Research Center and from the help of K. L. Chan in preparing the tables and figures.

## References

[1]Williams, F. W., Kennedy, D., Butler, R., and Anderson, M. S., "VICONOPT: Program for Exact Vibration and Buckling Analysis or Design of Prismatic Plate Assemblies," *AIAA Journal*, Vol. 29, No. 11, 1991, pp. 1927, 1928.

[2]Dawe, D. J., and Craig, T. J., "Buckling and Vibration of Shear Deformable Prismatic Plate Structures by a Complex Finite Strip Method," *International Journal of Mechanical Sciences*, Vol. 30, No. 2, 1988, pp. 77–99.

[3]Anderson, M. S., and Kennedy, D., "Inclusion of Transverse Shear Deformation in the Exact Buckling and Vibration Analysis of Composite Plate Assemblies," NASA CR-4510, May 1993.

[4]Wittrick, W. H., and Williams, F. W., "Buckling and Vibration of Anisotropic or Isotropic Plate Assemblies Under Combined Loadings," *International Journal of Mechanical Sciences*, Vol. 16, No. 4, 1974, pp. 209–239.

[5]Anderson, M. S., Williams, F. W., and Wright, C. J., "Buckling and Vibration of any Prismatic Assembly of Shear and Compression Loaded Anisotropic Plates with an Arbitrary Supporting Structure," *International Journal of Mechanical Sciences*, Vol. 25, No. 8, 1983, pp. 585–596.

[6]York, C. B., Williams, F. W., Kennedy, D., and Butler, R., "A Parametric Study of Optimum Designs for Benchmark Stiffened Wing Panels," *Composites Engineering*, Vol. 3, Nos. 7–8, 1993, pp. 619–632.

[7]Ambur, D. R., Starnes, J. H., Jr., and Prasad, C. B., "Low-Speed Impact Damage-Initiation Characteristics of Selected Laminated Composite Plates," *AIAA Journal*, Vol. 33, No. 10, 1995, pp. 1919–1925.